Supporting Information

Cu-based catalysts with the co-existence of single atoms and nanoparticles for basic electrocatalytic oxygen reduction reactions

Huimin Liu,[a] Qiong Jin,[a] Lingzhe Meng,[a] Hongfei Gu,[a] Xiao Liang,[b] Yu Fan,[a] Zhi Li,[c] Fang Zhang,[d] Hongpan Rong,[*a] and Jiatao Zhang[*e]

[a.] Beijing Key Laboratory of Construction-Tailorable Advanced Functional Materials and Green Applications, School of Materials Science & Engineering, Beijing Institute of Technology, Beijing 100081 (P. R. China).

[b.] Department of Chemistry, Tsinghua University, Beijing 100084, (P. R. China).

[c.] College of Chemistry, Beijing Normal University, Beijing 100875 (P. R. China).

[d.] Analysis and Testing Center, Beijing Institute of Technology, Beijing 100081 (P. R. China)

[e.] School of Chemistry and Chemical Engineering, Beijing Institute of Technology, Beijing 100081 (P. R. China).

E-mail: rhp@bit.edu.cn., zhangjt@bit.edu.cn.

Experimental

Chemicals and Materials.

All reaction reagents and chemicals were obtained and used without further purification. Bismuth nitrate pentahydrate ($Bi(NO_3)_3 \cdot 5H_2O$), 20 wt% commercial Pt/C were purchased from Aladdin. $Cu(NO_3)_2 \cdot 3H_2O$, methanol anhydrous (CH_3OH or MeOH), 1,3,5-benzene tricarboxylic acid (H_3BTC) were purchased from Sinopharm Chemical Reagent Co. Ltd. N, N-dimethylformamide (DMF) and potassium hydroxide (KOH) were purchased from Tianjin Zhiyuan Reagent Co., Ltd. Isopropyl alcohol was purchased from Shanghai Chemical Reagent Co. Ltd. Nafion (5 wt%) was purchased from Sigma-Aldrich. Dicyandiamide (DCD) was purchased from Macklin.

Materials Synthesis.

Synthesis of BiCu-MOF, Bi-MOF, and Cu-BTC. The BiCu-MOF was synthesized by a modified solvothermal method reported in the literature[1, 2]. H_3BTC (750 mg), $Bi(NO_3)_3 \cdot 5H_2O$ (150 mg), and $Cu(NO_3)_2 \cdot 3H_2O$ (2.9 mg) were dissolved in a 60 mL mixed solvent containing MeOH/DMF (1:4, v/v), followed by 10 min ultra-sonication. The resulting homogeneous solution was transferred to a Teflon-lined stainless-steel autoclave. After the autoclave was sealed and then heated at 120 °C for 24 h in an oven, it was cooled to room temperature. The product was collected by centrifugation and washed several times with MeOH, and then dried in a vacuum oven at 60 °C to obtain the light blue powder. The synthesis of Bi-MOF was similar to the above method, except that $Cu(NO_3)_2 \cdot 3H_2O$ was not added. The precursor of Cu/CN, Cu-BTC, was synthesized by grinding a mixture of $Cu(NO_3)_2 \cdot 3H_2O$ and H_3BTC.

Synthesis of $Cu_{SA}Cu_{NP}$/BiCN, Bi/CN, Cu/CN. The as-prepared BiCu-MOFs and dicyandiamide (DCD) were respectively placed in two porcelain boats with a mass ratio of 1:2 and heated to 1000 °C for 4 h in a stream of Ar. Pyrolysis of Bi-MOF and Cu-BTC to Bi/CN and Cu/CN was consistent with the above method.

Electrocatalytic Measurements

The electrochemical ORR performance of the catalysts was measured on the electrochemical workstation (760E, CH Instrument) at room temperature with a standard 3-electrode system. An Ag/AgCl (saturated KCl solution) and a graphene rod served as the reference and counter electrodes, respectively. According to the Nernst equation ($E_{RHE} = E_{Ag/AgCl} + 0.197\ V + 0.0591 \times pH$), all measured potentials were converted to standard reversible hydrogen electrodes (RHE). The working electrode was a rotating disk electrode (RDE, 0.196 cm^2) or a rotating ring-disk electrode (RRDE, 0.196 cm^2), and the electrolyte was 0.1 M KOH.

The electrocatalysis ink was prepared as follows. 3 mg of the catalysts were mixed with 770 μL of isopropanol / deionized water (1:1, v/v) and 30 μL 5 wt% Nafion solution. The mixture was then sonicated for 30 min to form a homogeneous black ink. Next, 10 μL of ink was dropped onto the electrode and dried under an infrared lamp. The catalyst loading amount was 0.19 mg cm^{-2}.

Cyclic voltammetry (CV) was performed in Ar- and O_2-saturated 0.1 M KOH solution with a sweep rate of 100 mV s^{-1}. Linear sweep voltammetry (LSV) was measured in an O_2-saturated 0.1 M KOH solution with a sweep rate of 5 mV s^{-1}. RRDE tests were conducted at different rotating speeds from 400 to 1600 rpm. Half-wave potential ($E_{1/2}$) referred to the potential corresponding to half of the limiting current density in LSV curves. The Koutecky−Levich (K−L) equation was used to calculate the electron transfer number:

$$\frac{1}{J}=\frac{1}{J_K}+\frac{1}{0.201nFC_0D_0^{2/3}\nu^{-1/6}\omega^{1/2}}$$

where J is the measured disk current density, J_K is the kinetic limiting current density, n is the electron transfer number, F is the Faraday constant (96485 C mol^{-1}); C_0 and D_0 represent the saturated concentration, and diffusion coefficient of O_2 in the 0.1 M KOH, respectively; ν is the kinetic viscosity of the electrolyte (0.01 cm^2 s^{-1}), and ω represents the angular velocity (rpm). In 0.1 M KOH solution: $C_0 = 1.2 \times 10^{-3}$ mol L^{-1}, $D_0 = 1.9 \times 10^{-5}$ cm^2 s^{-1}.[3]

RRDE tests were conducted to investigate the four-electron selectivity of the as-prepared samples. The electron transfer number (n) and H_2O_2 yield were calculated by the following equations:

$$n = 4 \times \frac{I_d}{I_d + {}^{I_r}/_{N}}$$

$$H_2O_2(\%) = 200 \times \frac{{}^{I_r}/_{N}}{I_d + {}^{I_r}/_{N}}$$

where I_d is the disk current, I_r is the ring current, and N is the current collection efficiency of the platinum ring (N=0.37).

The ORR stability of the electrocatalysts in the O_2-staurated 0.1 M KOH solution was examined by using chronoamperometry at a potential of 0.45 V (vs. RHE) in O_2-staurated 0.1 M KOH.

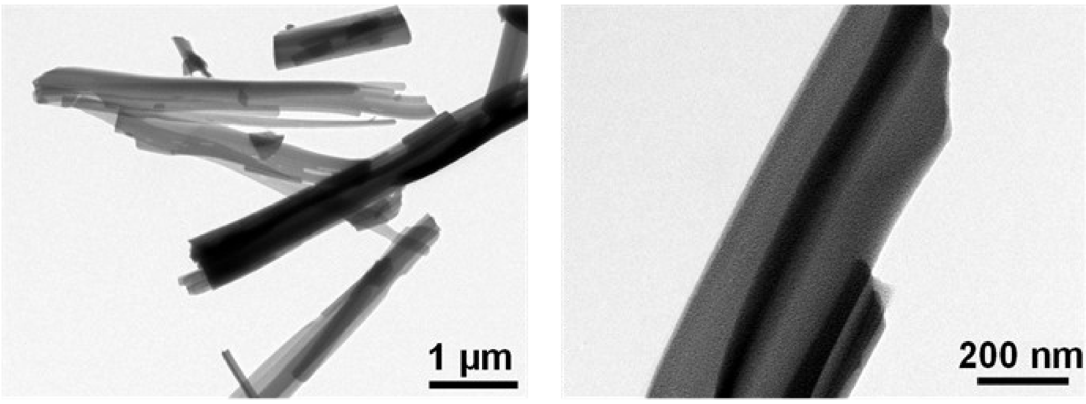

Figure S1. TEM images of Bi-MOFs.

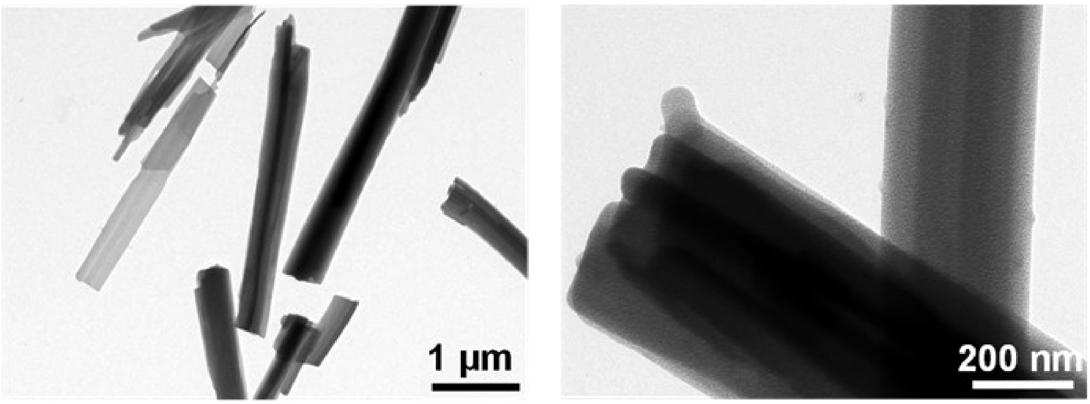

Figure S2. TEM images of BiCu-MOFs.

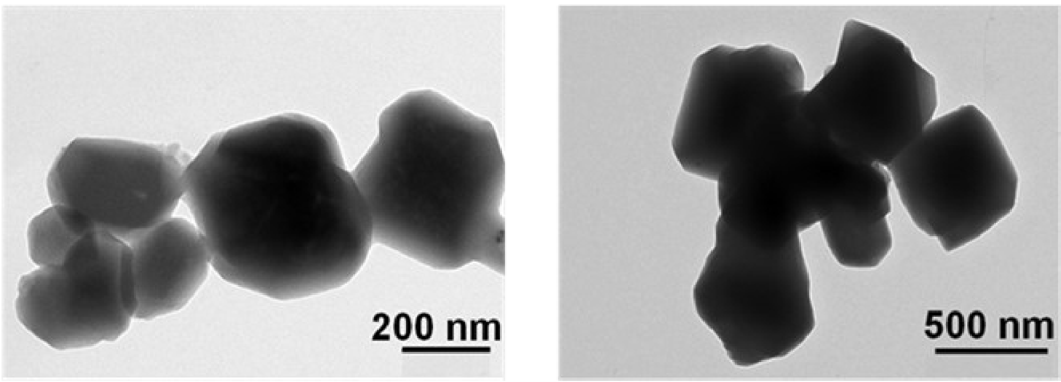

Figure S3. TEM images of Cu-BTC.

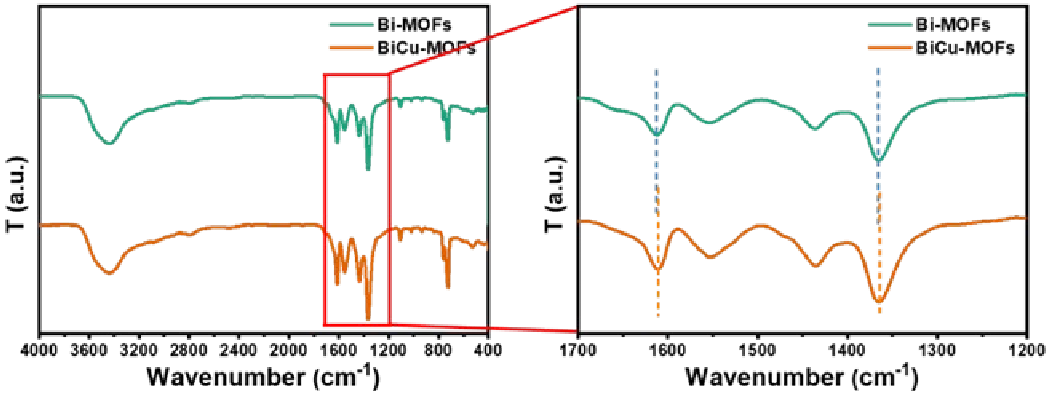

Figure S4. FT-IR patterns of Bi-MOF and BiCu-MOF.

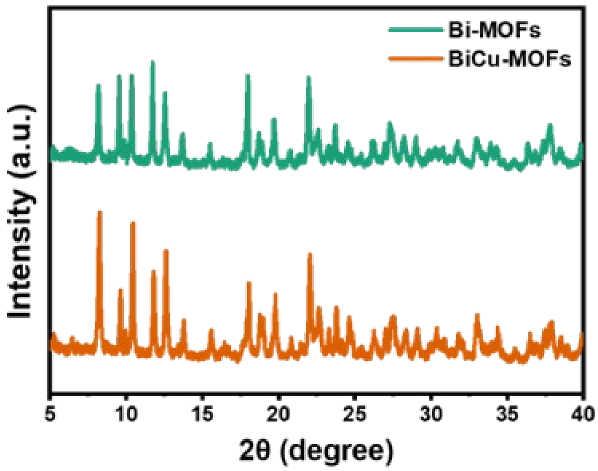

Figure S5. XRD patterns of Bi-MOF and BiCu-MOF.

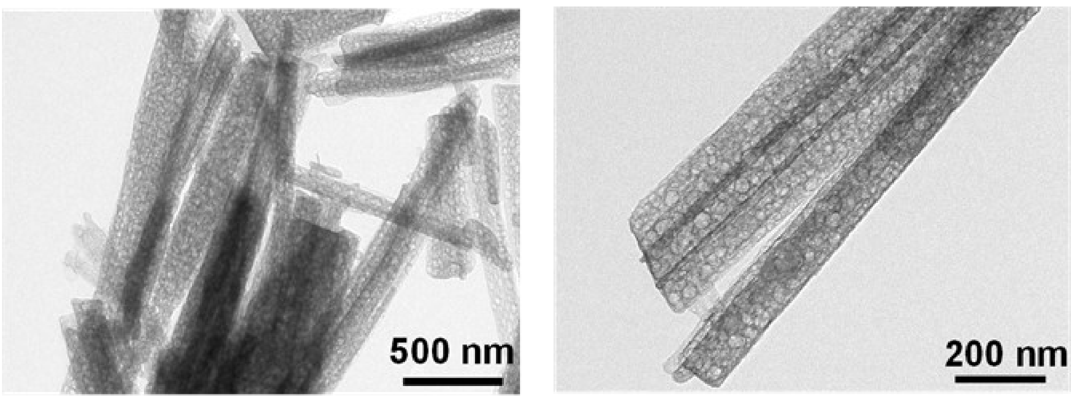

Figure S6. TEM images of $Cu_{SA}Cu_{NP}$/BiCN.

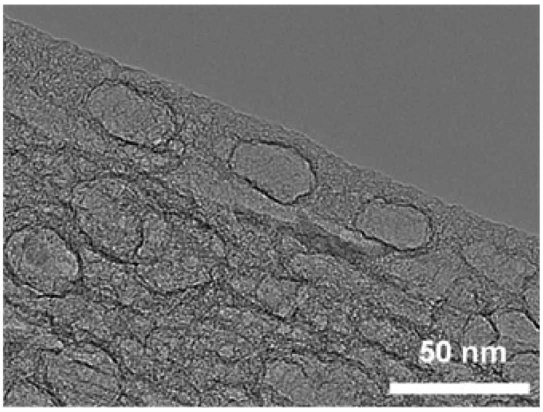

Figure S7. HRTEM image of $Cu_{SA}Cu_{NP}$/BiCN.

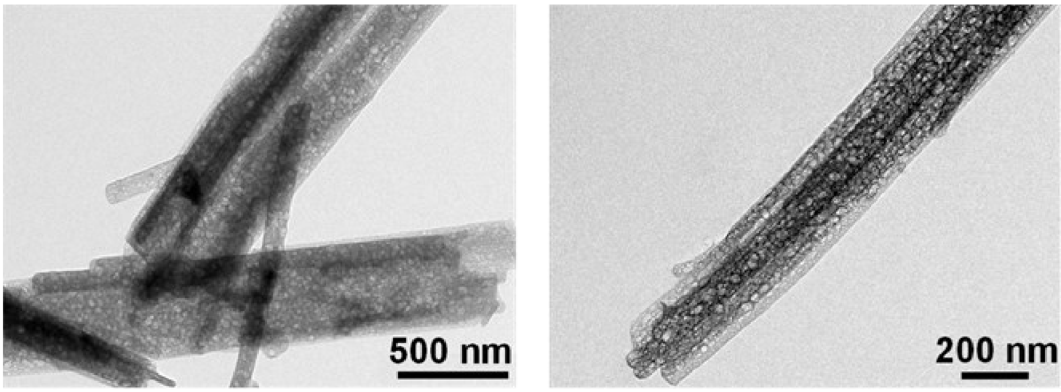

Figure S8. TEM images of Bi/CN.

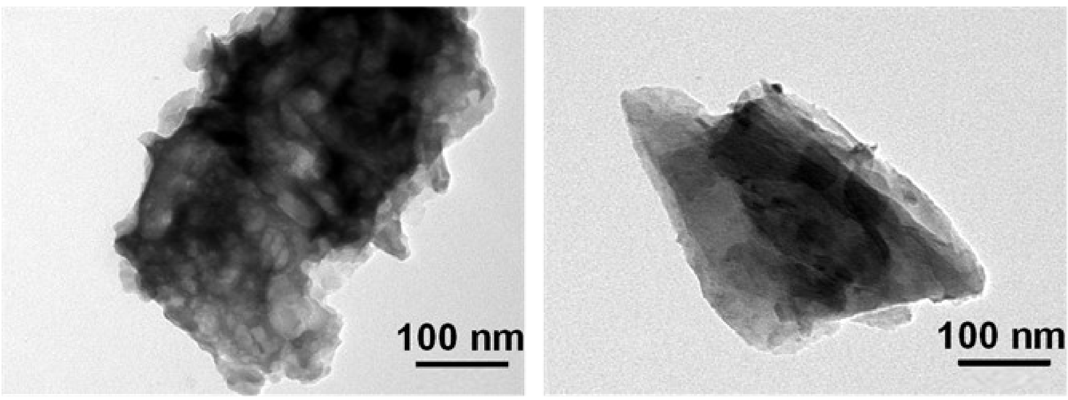

Figure S9. TEM images of Cu/CN.

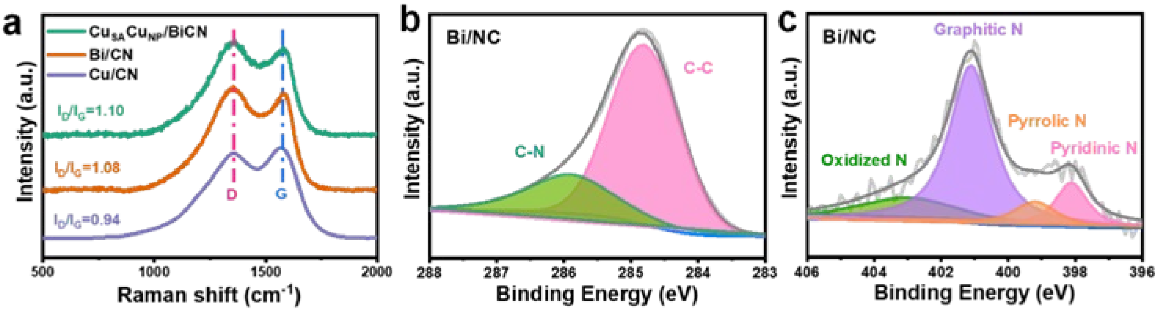

Figure S10. (a) Raman spectra of $Cu_{SA}Cu_{NP}$/BiCN, Bi/CN, and Cu/CN. (b) C1s and (c) N1s XPS spectra of Bi/CN.

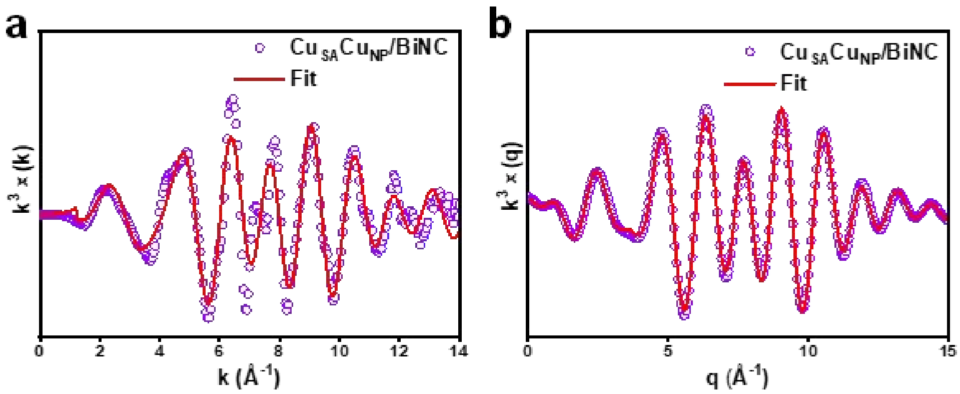

Figure S11. EXAFS and fitting spectra in（a）k space and (b) q space of $Cu_{SA}Cu_{NP}$/BiCN.

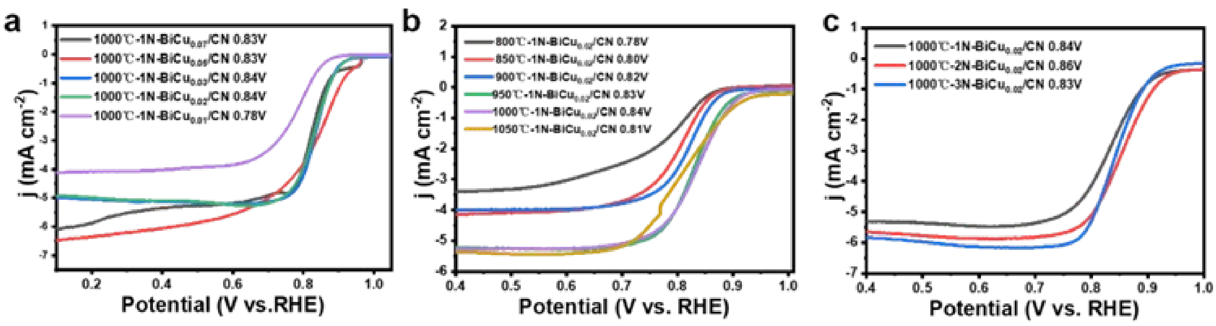

Figure S12. LSV curves of BiCu-catalysts with different (a) Bi/Cu feeding ratios, (b) pyrolysis temperatures, and (c) the quality of DCD.

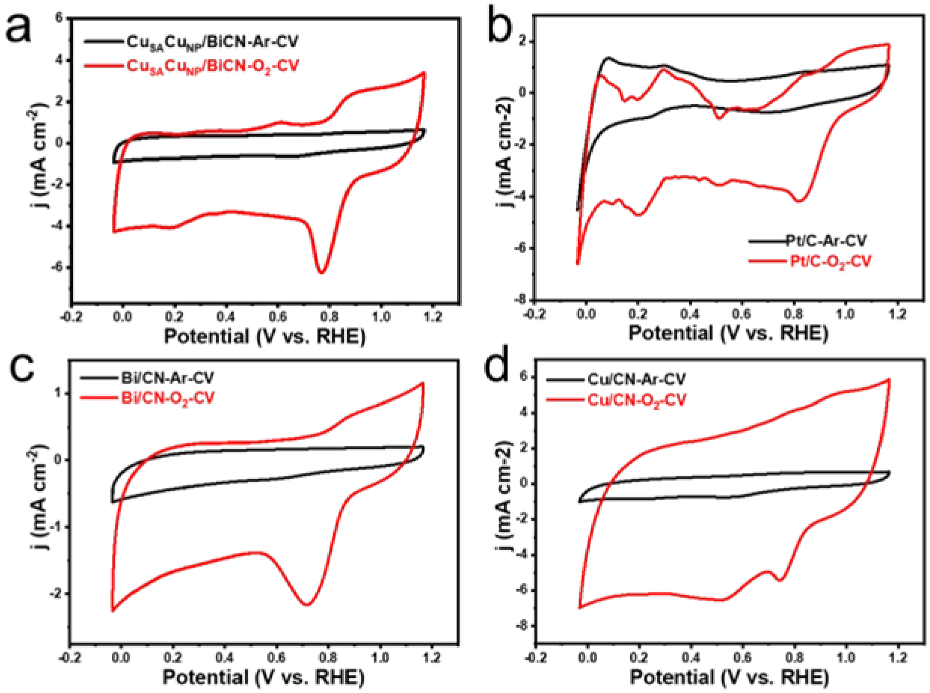

Figure S13. CV curves of (a) Cu$_{SA}$Cu$_{NP}$/BiCN, (b) Pt/C, (c) Bi/CN, and (d) Cu/CN in Ar-saturated and O_2-saturated 0.1 M KOH solution.

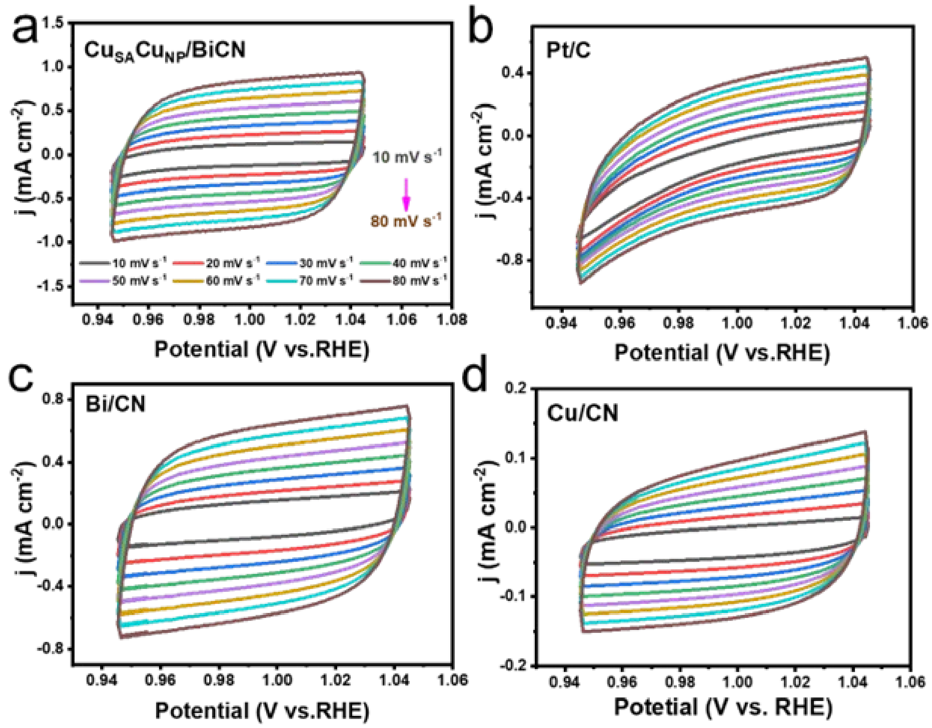

Figure S14. CV curves for (a) Cu$_{SA}$Cu$_{NP}$/BiCN, (b)Pt/C, (c) Bi/CN, and (d) Cu/CN at various scan rates of 10~80 mV s^{-1}.

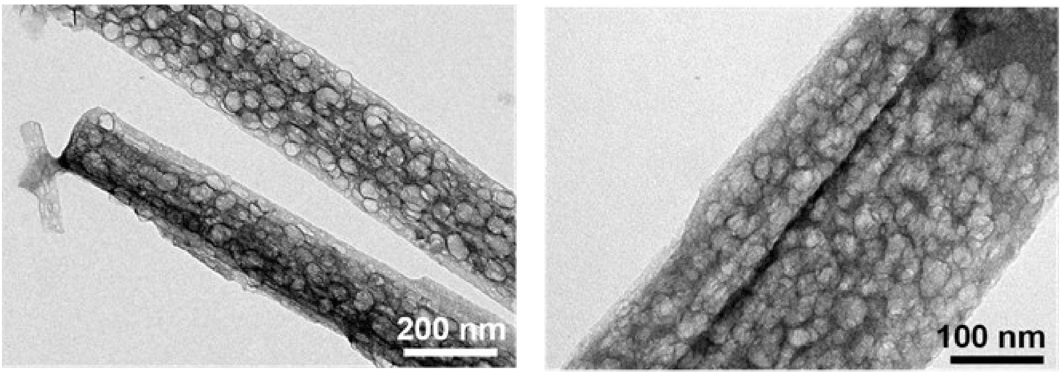

Figure S15. TEM images of $Cu_{SA}Cu_{NP}$/BiCN after a long-time stability test.

Table S1. The amount of C, N, O, Bi, and Cu in $Cu_{SA}Cu_{NP}$/BiNC from EDS analysis.

Elements	Atom ratio (at. %)
C	88.60
N	2.27
O	5.40
Bi	0.01
Cu	33.73

Table S2. The amount of Bi, Cu in Bi/CN and $Cu_{SA}Cu_{NP}$/BiCN from ICP-OES.

Samples	Elements	Mass ratio (wt. %)
Bi/CN	Bi	0.04
$Cu_{SA}Cu_{NP}$/BiCN	Bi	0.03
$Cu_{SA}Cu_{NP}$/BiCN	Cu	2.96

Table S3. The specific values of surface area and pore size of Bi/CN, $Cu_{SA}Cu_{NP}$/BiCN and Cu/CN.

Samples	$a_{s,BET}$ (m^2 g^{-1})	Mean pore diameter (nm)	Total pore volume (cm^3 g^{-1})
Bi/CN	1319.5	7.99	2.6
$Cu_{SA}Cu_{NP}$/BiCN	626.2	8.84	1.4
Cu/CN	262.3	12.3	0.8

Table S4. Best fitting EXAFS data for $Cu_{SA}Cu_{NP}$/BiCN.

sample	Scattering pair	N	R(Å)	$\sigma^2(10^{-3}Å^2)$	ΔE_0(eV)	R factor
$Cu_{SA}Cu_{NP}$/BiCN	Cu-N	1.9	1.88	7.38	5.64	0.005
	Cu-Cu	3.2	2.55	4.40		

Table S5. Summary of the half-wave potential and limiting current density of some recently reported ORR catalysts

Catalyst	$E_{1/2}$/V vs. RHE	J_L/mA cm^{-2}	Reference
$Cu_{SA}Cu_{NP}$/BiCN	0.86	5.82	This work
Cu@Cu-N-C	0.83	5.3	[4]
SA-Cu/NG	0.856	5.6	[5]
(Cu-N-C/GC)	0.84	6.2	[6]
Cu/N/C	0.75	4.7	[7]
Cu-BTT	0.778	4.17	[8]
Cu SAs/NC-900	0.88	5.5	[9]
CuN_2C_2	0.863	6.1	[10]
FeN_3S	0.86	5.8	[11]
Fe/OES	0.85	6.3	[12]
C-Se-C	0.85	5.53	[13]
Fe-IICSAC	0.908	5.5	[14]
Fe_3C@NCNTs	0.84	5.8	[15]
Ni-SiNC	0.866	5.8	[16]
CoSA-C_2N	0.87	7.9	[17]
Fe/N-PCNs	0.86	5.7	[18]

Reference

1. E. Zhang, T. Wang, K. Yu, J. Liu, W. Chen, A. Li, H. Rong, R. Lin, S. Ji, X. Zheng, Y. Wang, L. Zheng, C. Chen, D. Wang, J. Zhang and Y. Li, *J. Am. Chem. Soc.*, 2019, **141**, 16569-16573.
2. L. Meng, E. Zhang, H. Peng, Y. Wang, D. Wang, H. Rong and J. Zhang, *ChemCatChem*, 2022, **14**, e202101801.
3. H. Li, Y. Wen, M. Jiang, Y. Yao, H. Zhou, Z. Huang, J. Li, S. Jiao, Y. Kuang and S. Luo, *Adv. Funct. Mater.*, 2021, **31**, 2011289.
4. X. Chen, L. Ma, W. Su, L. Ding, H. Zhu and H. Yang, *Electrochim. Acta*, 2020, **331**, 135273.
5. L. Yang, H. Xu, H. Liu, X. Zeng, D. Cheng, Y. Huang, L. Zheng, R. Cao and D. Cao, *Research*, 2020, **2020**, 302-313.
6. G. Xing, M. Tong, P. Yu, L. Wang, G. Zhang, C. Tian and H. Fu, *Angew. Chem. Int. Ed.*, 2022, **134**, e202211098.
7. Q. Wang, Z. Zhang, M. Wang, F. Liu, L. Jiang, B. Hong, J. Li and Y. Lai, *Nanoscale*, 2018, **10**, 15819-15825.
8. P. Mani, S. Devadas, T. Gurusamy, P. E. Karthik, B. P. Ratheesh, K. Ramanujam and S. Mandal, *Chem.–Asian J.*, 2019, **14**, 4814-4818.
9. S. Ma, Z. Han, K. Leng, X. Liu, Y. Wang, Y. Qu and J. Bai, *Small*, 2020, **16**, 2001384.
10. G. Han, X. Zhang, W. Liu, Q. Zhang, Z. Wang, J. Cheng, T. Yao, L. Gu, C. Du, Y. Gao and G. Yin, *Nat. Commun.*, 2021, **12**, 6335.
11. M. Wang, W. Yang, X. Li, Y. Xu, L. Zheng, C. Su and B. Liu, *ACS Energy Letters*, 2021, **6**, 379-386.
12. C. C. Hou, L. Zou, L. Sun, K. Zhang and Q. Xu, *Angew. Chem. Int. Ed.*, 2020, **59**, 7454-7459.
13. H. Hu, J. Wang, B. Cui, X. Zheng, J. Lin, Y. Deng and X. Han, *Angew. Chem. Int. Ed.*, 2022, **61**, e202114441.
14. S. Ding, Z. Lyu, H. Zhong, D. Liu, E. Sarnello, L. Fang, M. Xu, M. H. Engelhard, H. Tian and T. Li, *Small*, 2020, **17**, 2004454.
15. C. Xu, C. Guo, J. Liu, B. Hu, J. Dai, M. Wang, R. Jin, Z. Luo, H. Li and C. Chen, *Energy Storage Mater.*, 2022, **51**, 149-158.
16. F. Wang, Y. Li, R. Zhang, H. Liu, Y. Zhang, X. Zheng, J. Zhang, C. Chen, S. Zheng and H. Xin, *Small*, 2022, **19**, 2206071.
17. W. Xu, Y. Sun, J. Zhou, M. Cao, J. Luo, H. Mao, P. Hu, H. Gu, H. Zhai, H. Shang and Z. Cai, *Nano Research*, 2023, **16**, 2294-2301.
18. L. Zheng, S. Yu, X. Lu, W. Fan, B. Chi, Y. Ye, X. Shi, J. Zeng, X. Li and S. Liao, *ACS Appl. Mater. Inter.*, 2020, **12**, 13878-13887.